

Tableau 4. Comparaison des angles de torsion τ_3 et τ_4 définissant l'orientation de la chaîne acétique par rapport au noyau benzénique pour quelques acides propioniques dont la structure cristalline est connue

	τ_3 ($^{\circ}$)	τ_4 ($^{\circ}$)
ACNP	148,8 (2)	114,7 (2)
CHINCA (molécule A)	61,8 (8)	-74,4 (8)
CHINCA (molécule B)	38,2 (8)	-86,5 (8)
FLUBIP	107,7 (6)	77,3 (6)
IBPRAC	96,4 (2)	89,3 (2)
IPMIAC (molécule A)	-79,7 (6)	-102,2 (6)
IPMIAC (molécule B)	63,2 (6)	109,7 (6)
Valeurs calculées (CNDO/2 et STD 3G) correspondant au minimum énergétique		
Acide phénylacétique	± 90	± 90
Acide phényl-2 propionique	$\pm 60, \pm 120$	± 90

Tableau 5. Distances intermoléculaires inférieures à 3,5 Å entre atomes non-hydrogène

Code de symétrie: (i) 1 - $x, -y, 1 - z$; (ii) 2 - $x, -y, 1 - z$.			
C(15)-O(1) ⁱ	3,311 (2) Å	O(1)-O(2) ^{ii*}	2,659 (2) Å
C(16)-O(1) ⁱ	3,385 (2)	O(1)-O(1) ⁱⁱ	3,220 (2)
C(19)-O(1) ⁱⁱ	3,325 (2)		

* Liaison hydrogène.

la valeur de τ_3 , plus élevée (148,8°) que dans les autres composés. Dans CHINCA, la chaîne acétique est bloquée par la présence de l'indane, ce qui explique la valeur faible $\tau_3 = 38,2^{\circ}$. Dans les trois autres composés, la rotation du CH_3 est plus libre et les valeurs de τ_3 confirment les résultats de l'analyse conformationnelle. En ce qui concerne τ_4 , les variations observées autour de la valeur attendue $\pm 90^{\circ}$ sont la conséquence des liaisons hydrogène auxquelles partici-

pent les atomes d'oxygène dans chacune des structures. C'est le cas pour ACNP (Tableau 5) où la cohésion du cristal est assurée par la liaison hydrogène O(2)H...O(1) formant une dimerisation autour du centre de symétrie. Il y a en outre quelques liaisons de van der Waals.

Les auteurs remercient MM les Professeurs J. Toussaint et C. L. Lapierre pour leur intérêt pour ce travail ainsi que M Marcel Vermeire pour son assistance technique.

Références

- DIVE, G. (1979). Thèse. Faculté de Médecine, Univ. de Liège.
 FLIPPEN, J. L. & GILARDI, R. D. (1975). *Acta Cryst.* B31, 926-928.
 FOULON, M., BAERT, F., FOURET, R., BRIENNE, M. J. & JACQUES, J. (1979). *Acta Cryst.* B35, 2058-2062.
 GILLET, C., DEHOUX, E., KESTENS, J., ROBA, J. & LAMBELLIN, C. (1976). *Eur. J. Med. Chem. Chim. Ther.* 11, 173-181.
 JUBY, P. F., GOODWIN, W. R., HUDYMA, T. W. & PARTYKA, R. A. (1972). *J. Med. Chem.* 15, 1297-1310.
 KAMIYA, K., WADA, Y. & NISHIKAWA, M. (1975). *Chem. Pharm. Bull.* 23, 1589-1595.
 MCCONNELL, J. F. (1974). *Cryst. Struct. Commun.* 3, 73-75.
 MAIN, P., FISKE, S. J., HULL, S. E., LESSINGER, L., GERMAIN, G., DECLERCQ, J. P. & WOOLFSON, M. M. (1980). *MULTAN 80. A System of Computer Programs for the Automatic Solution of Crystal Structures from X-ray Diffraction Data*. Univs. de York, Angleterre. et Louvain-La-Neuve, Belgique.
 SHELDICK, G. M. (1976). *SHELX 76*. Programme pour la détermination de structures cristallines. Univ. de Cambridge, Angleterre.

Acta Cryst. (1982). B38, 2411-2419

Structures of Triclinic and Monoclinic Cholesterol Hemieethanolate

BY HUEY-SHENG SHIEH,* LAURENCE G. HOARD† AND C. E. NORDMAN

Department of Chemistry, University of Michigan, Ann Arbor, Michigan 48109, USA

(Received 1 February 1982; accepted 30 March 1982)

Abstract

Cholesterol hemiethanolate ($\text{C}_{27}\text{H}_{46}\text{O} \cdot \frac{1}{2}\text{C}_2\text{H}_5\text{OH}$, $M_r = 409.70$) crystallizes in a triclinic (I) and a monoclinic

* Present address: Physical Sciences Center, Monsanto Company, St Louis, Missouri 63166, USA.

† Present address: International Paper Co., Corporate Research & Development Division, PO Box 797, Tuxedo Park, New York 10987, USA

(II) form. (I) belongs to space group $P\bar{1}$ with $a = 12.787 (2)$, $b = 35.310 (11)$, $c = 12.225 (1)$ Å, $\alpha = 97.80 (2)$, $\beta = 100.40 (2)$, $\gamma = 99.06 (2)^{\circ}$; $V = 5284 (2)$ Å 3 , $Z = 8$, $D_x = 1.030$ Mg m $^{-3}$, $\mu(\text{Cu} K\alpha, \lambda = 1.5418$ Å) = 0.46 mm $^{-1}$; (II) to space group $P2_1$ with $a = 12.775 (2)$, $b = 68.668 (15)$, $c = 12.213 (2)$ Å, $\beta = 100.43 (1)^{\circ}$; $V = 10537 (3)$ Å 3 , $Z = 16$, $D_x = 1.033$ Mg m $^{-3}$, $\mu(\text{Cu} K\alpha, \lambda = 1.5418$ Å) = 0.46 mm $^{-1}$. Patterson-search methods were used in the solution of

both structures. (I) was refined to $R = 0.095$ for 7291 observed [$I > 1.2\sigma(I)$] reflections, (II) to $R = 0.106$ for 6093 observed [$I > 1.2\sigma(I)$] reflections. The bilayer structures have alternating hydrophobic and hydrophilic layers; in the latter the cholesterol and ethanol molecules are joined into hydrogen-bonded chains. Both (I) and (II) exhibit translational pseudosymmetry within their asymmetric units, whereby one pair of cholesterol molecules is related to another pair by an approximate $a/2$ translation, while the third and fourth pairs are related by an approximate $c/2$ translation. This pseudosymmetry is similar to, but less closely obeyed than, the pseudosymmetry in cholesterol monohydrate. The structure of the asymmetric unit of (II) is almost identical to the structure of the unit cell of (I). The lateral packing of cholesterol molecules in these structures is closely similar to that in cholesterol monohydrate.

Introduction

The crystallography of cholesterol is remarkable in several respects. One is the tendency of cholesterol to crystallize with several molecules in the crystallographic asymmetric unit. Another is the local pseudosymmetry exhibited by these structures. Cholesterol monohydrate (Craven, 1976, 1979) and anhydrous cholesterol (Shieh, Hoard & Nordman, 1977a, 1981) are the two forms of cholesterol so far described in detail. Both are triclinic (space group $P\bar{1}$) with eight independent molecules per cell. Both structures possess closely obeyed local pseudosymmetry, but the nature of this pseudosymmetry is quite different in the two structures (Craven, 1979). We report here the structure solutions and the refined structures of two forms of cholesterol hemiethanolate, and discuss their relationship to the other forms of cholesterol, especially the monohydrate.

Experimental

Crystals of the triclinic form of cholesterol hemiethanolate (I) were first obtained by slow evaporation of ethanol-water solutions, and were initially thought to be a new form of cholesterol monohydrate (Shieh, Hoard & Nordman, 1977b). (I) can also be crystallized from ether-absolute ethanol solutions, while a monoclinic form (II) tends to form from solutions in ether-95% ethanol, or by diffusion of 50% aqueous ethanol into an ether-absolute ethanol solution of cholesterol.

X-ray data were collected on a Syntex $P\bar{1}$ diffractometer with graphite-monochromatized $\text{Cu K}\alpha$ radiation. For each crystal form specimens of approximate dimensions $0.4 \times 0.3 \times 0.15$ mm were used, and

the 2θ range up to 100° was covered. The data sets contained a high proportion of weak reflections, a manifestation of pseudosymmetry, and also of strong thermal motion in these structures, which in this latter regard resemble both cholesterol monohydrate (Craven, 1979) and cholesterol (Shieh, Hoard & Nordman, 1981). For (I) a total of 10877 unique reflection intensities (I) were measured of which 7295 exceeded $1.2\sigma(I)$, and 5650 exceeded $2.33\sigma(I)$. For (II) the total was 11008; of these, 6095 exceeded $1.2\sigma(I)$ and 4218 exceeded $2.33\sigma(I)$. Both data sets were corrected for a slight crystal decay of about 10%, as indicated by the intensities of three standard reflections. Absorption corrections were not applied.

Structure determination and refinement

An unusual intensity distribution was found in both data sets, in that reflections with both h and l odd tended to be weak. A more extreme but otherwise similar situation was observed by Craven (1976, 1979) in cholesterol monohydrate, and shown by him to result from translational pseudosymmetry within the unit cell. Specifically, if one quarter of the asymmetric unit is related to another quarter by an approximate $a/2$ translation, then the contribution of these two quarters to reflections with odd h will be weak. If the third quarter is similarly related to the fourth by a $c/2$ translation, then the contribution of these quarters to reflections with odd l will be weak. If both conditions apply, all reflections with both h and l odd will be weak. It was assumed, then, that the observed intensity pattern indicated the presence of this approximate translational pseudosymmetry in both (I) and (II).

The structure of (I) was solved by Patterson-search methods (Schilling, 1970) before the data collection was completed. The 2744 reflections with $2\theta < 60^\circ$ were used to compute a point-atom origin-removed Patterson function, exponentially damped to 0.5 at the $\sin \theta/\lambda$ limit. High peaks at $(0,0,0.5)$ and $(0.5,0,0)$ in the Patterson function confirmed the presence of the above-mentioned pseudosymmetry.

The steroid portion of the molecule, consisting of the O atom and carbons 1 to 20 (Fig. 4) was used as a known rigid group in the Patterson search. Rotation searches, performed with the intra-group vector set, were not immediately successful, as the vector overlap of the eight independent roughly parallel molecules makes the Patterson function extremely dense in the near-origin region.

A modified rotation search which capitalizes on the translational pseudosymmetry was tried next. If two molecules are related to each other by a pure translation, then the intermolecular vector set is identical to the intramolecular vector set, translated by the molecule-molecule translation vector. This means

that the orientation of a pair of molecules related by $a/2$ can be searched for by rotating the intramolecular vector set about the point (0.5,0,0) in the Patterson function. Similarly pairs related by $c/2$ are oriented by a search about (0,0,0.5). Since the Patterson function is far less crowded in these regions, these searches were quite unambiguous. Relative translational parameters were now found by means of translational Patterson searches, aided by packing considerations. The triangulation technique for finding internally consistent translation vectors among three symmetrically unrelated and correctly oriented molecules was found useful, as it was in the study of cholesterol (Shieh, Hoard & Nordman, 1981). In this manner a partial structure was deduced, consisting of four 21-atom steroid groups.

The remaining four steroid groups were found by Fourier syntheses. The interpretation of these initially poorly phased electron density maps was greatly facilitated by computer search for the steroid groups. Such a search is computationally equivalent to a Patterson search, but the search probe is a set of atomic position vectors rather than interatomic vectors, and the function searched is a Fourier instead of a Patterson.

Least-squares refinement was begun with a 168-atom model consisting of the eight steroid fragments. The remaining 68 C and O atoms, those of the side chains and the ethanol, were not included. The Gauss-Seidel group-refinement program *FGLS* was used (Hoard & Nordman, 1979). The steroid fragments were initially treated as rigid groups, later as flexible, with elastic first- and second-neighbor distance restraints. The isotropic atomic thermal parameters were treated as elastically restrained to those of neighboring atoms. This model ultimately refined to $R = 0.27$. Fourier syntheses now successively revealed the side-chain carbons and the four ethanol molecules, the latter identifying the crystals as a hemiethanolate rather than a monohydrate. The outer parts of the cholesterol side chains proved most elusive, as their thermal motion is very strong.

Refinement with the full data set ($2\theta \leq 100^\circ$) was continued using the least-squares program *CLS* (Schilling, 1970) in the block-diagonal mode. Atom coordinates and anisotropic parameters were refined in 9×9 blocks. Those 292 H atoms bonded to C atoms 1 through 22 of the cholesterol molecules or to the ethanol C atoms, were included in calculated positions, with isotropic B 's equal to 1.1 times those of the adjacent C, but not less than 6.0 \AA^2 . The H atom parameters were not refined. To optimize the ratio of data to parameters reflections with intensities down to $1.2\sigma(I)$ were included as 'observed'. The relatively high R values reflect this inclusion of a very large proportion of weak reflections. Least-squares weights were taken as $w = (\sigma^2 + kF_o^2)^{-1}$, where $k = 9.3 \times 10^{-3}$ was chosen

to make $w(\Delta F)^2$ uniformly distributed in $|F_o|$. No extinction correction was applied, but the four reflections expected to suffer most from secondary extinction (Zachariasen, 1968), namely 002, 020, 212 and 200, were omitted from the refinement. In the last few cycles only the ends of the side chains C(23), ..., C(27) of the eight molecules were refined. The chains of pairs of molecules related to one another by the translational pseudosymmetry were included in the same matrix block. That is, the 40 atoms were refined, anisotropically, as four ten-atom blocks. This treatment was found to improve the chain geometry and the reasonableness of the thermal parameters. The final R value was 0.095 for the 7291 reflections included.

The solution of the monoclinic structure (II) was remarkably straightforward. The lattice parameters a , c and β of the two cells are very nearly equal, and the cell volume of (II) is almost exactly twice that of (I). This suggested that the unit cell of (II) consists of, in effect, two cells of (I) related to one another by the monoclinic 2_1 screw axis. If this were the case the triclinic cell would become the monoclinic asymmetric unit, and the structure determination would reduce to a two-parameter problem. The only unknowns would be the x and z displacements of the asymmetric unit in the plane perpendicular to the 2_1 axis.

This was explored by means of a Patterson translation search based on the first 2229 (low resolution) data collected. The 68-atom search group was taken as four 17-atom steroid skeletons, omitting all but the four rings in each steroid. The four skeletons were chosen so as to avoid duplication by the translational pseudosymmetry. Limiting the search group in this way was done for reasons of computing economy.

The Patterson search yielded the (x,z) translation vector, which permitted a trial structure to be constructed and successfully refined. The least-squares refinement was by the methods described above. Those H atoms bonded to C atoms 1 to 22 of cholesterol, or to the ethanol C atoms, were included in calculated positions. Reflections with intensities down to $1.2\sigma(I)$ were included. Least-squares weights $w = (\sigma^2 + kF_o^2)^{-1}$ were used, with $k = 2.2 \times 10^{-3}$. Reflections 022 and 040 were given zero weight on account of secondary-extinction effects. The final R value was 0.106 for the 6093 observed reflections included.

Results and discussion

The atomic parameters for both structures are given in Table 1, with standard deviations estimated from the last least-squares refinement cycle.* The eight indepen-

* Lists of structure factors, anisotropic thermal parameters, and H-atom parameters have been deposited with the British Library Lending Division as Supplementary Publication No. SUP 36862 (98 pp.). Copies may be obtained through The Executive Secretary, International Union of Crystallography, 5 Abbey Square, Chester CH1 2HU, England.

Table 1. C and O atom parameters

Atoms are numbered conventionally as in Fig. 4; a molecule label (*A*, . . . , *H*) is attached to the atom name. Positional parameters are fractional coordinates ($\times 10^4$). E.s.d.'s refer to the last significant digit in the parameter value. $B_{eq} = \frac{1}{2} \sum_i \sum_j B_{ij} a_i^* a_j^* \mathbf{a}_i \cdot \mathbf{a}_j$.

Triclinic form

	<i>x</i>	<i>y</i>	<i>z</i>	B_{eq} (\AA^2)		<i>x</i>	<i>y</i>	<i>z</i>	B_{eq} (\AA^2)
O(3) <i>A</i>	3067 (8)	5222 (3)	2536 (9)	10.1 (4)	O(3) <i>B</i>	8039 (8)	5182 (3)	3056 (9)	9.7 (4)
C(1) <i>A</i>	3441 (9)	6266 (3)	2163 (9)	5.5 (4)	C(1) <i>B</i>	8513 (9)	6212 (3)	2546 (11)	6.8 (5)
C(2) <i>A</i>	3421 (10)	5831 (3)	1865 (11)	6.6 (5)	C(2) <i>B</i>	8547 (12)	5781 (4)	2344 (12)	8.1 (5)
C(3) <i>A</i>	3200 (10)	5648 (3)	2906 (11)	6.6 (5)	C(3) <i>B</i>	8071 (12)	5596 (4)	3268 (14)	9.7 (6)
C(4) <i>A</i>	2039 (11)	5694 (4)	3112 (11)	7.2 (5)	C(4) <i>B</i>	6954 (11)	5688 (4)	3350 (12)	8.5 (6)
C(5) <i>A</i>	2011 (8)	6142 (3)	3242 (9)	5.2 (4)	C(5) <i>B</i>	6914 (9)	6101 (3)	3419 (10)	5.6 (4)
C(6) <i>A</i>	1658 (10)	6305 (3)	4139 (10)	6.1 (4)	C(6) <i>B</i>	6491 (9)	6288 (4)	4205 (9)	6.0 (4)
C(7) <i>A</i>	1478 (8)	6714 (3)	4320 (8)	5.0 (4)	C(7) <i>B</i>	6339 (9)	6690 (3)	4353 (9)	5.2 (4)
C(8) <i>A</i>	1599 (9)	6924 (3)	3314 (9)	5.2 (4)	C(8) <i>B</i>	6573 (9)	6893 (3)	3381 (9)	5.2 (4)
C(9) <i>A</i>	2569 (9)	6824 (3)	2862 (9)	5.4 (4)	C(9) <i>B</i>	7551 (9)	6759 (4)	2953 (9)	6.0 (4)
C(10) <i>A</i>	2381 (9)	6376 (3)	2379 (9)	5.6 (4)	C(10) <i>B</i>	7370 (8)	6317 (3)	2582 (8)	4.4 (3)
C(11) <i>A</i>	2812 (10)	7072 (4)	1937 (10)	6.3 (4)	C(11) <i>B</i>	7918 (10)	7016 (4)	2075 (10)	6.6 (5)
C(12) <i>A</i>	2978 (8)	7513 (3)	2365 (9)	5.2 (4)	C(12) <i>B</i>	8073 (9)	7444 (3)	2426 (10)	5.9 (4)
C(13) <i>A</i>	2021 (9)	7607 (3)	2787 (8)	5.3 (4)	C(13) <i>B</i>	7012 (9)	7566 (3)	2768 (8)	5.1 (4)
C(14) <i>A</i>	1832 (9)	7374 (3)	3708 (8)	5.0 (4)	C(14) <i>B</i>	6776 (8)	7323 (3)	3701 (8)	4.8 (4)
C(15) <i>A</i>	976 (9)	7533 (3)	4262 (10)	6.0 (4)	C(15) <i>B</i>	5939 (9)	7527 (3)	4162 (10)	6.0 (4)
C(16) <i>A</i>	1252 (10)	7971 (3)	4171 (10)	6.2 (4)	C(16) <i>B</i>	6209 (11)	7954 (4)	3980 (12)	7.8 (5)
C(17) <i>A</i>	2137 (9)	8014 (3)	3481 (8)	4.8 (4)	C(17) <i>B</i>	7158 (10)	7971 (4)	3373 (10)	6.8 (5)
C(18) <i>A</i>	1012 (11)	7528 (4)	1800 (10)	7.1 (5)	C(18) <i>B</i>	6107 (10)	7484 (4)	1751 (10)	6.7 (5)
C(19) <i>A</i>	1513 (10)	6259 (4)	1284 (9)	6.7 (5)	C(19) <i>B</i>	6605 (11)	6171 (4)	1415 (10)	7.9 (5)
C(20) <i>A</i>	2186 (11)	8367 (4)	2871 (12)	7.8 (5)	C(20) <i>B</i>	7161 (14)	8326 (4)	2686 (12)	9.2 (6)
C(21) <i>A</i>	3133 (18)	8426 (5)	2277 (18)	14.0 (10)	C(21) <i>B</i>	8198 (16)	8358 (5)	2120 (15)	12.4 (9)
C(22) <i>A</i>	2124 (15)	8742 (4)	3619 (14)	11.1 (7)	C(22) <i>B</i>	7164 (15)	8695 (4)	3445 (14)	11.1 (7)
C(23) <i>A</i>	1964 (38)	9100 (8)	2991 (29)	22.7 (24)	C(23) <i>B</i>	7214 (19)	9069 (5)	2935 (18)	12.9 (9)
C(24) <i>A</i>	1037 (26)	9062 (7)	2112 (24)	15.6 (14)	C(24) <i>B</i>	6069 (21)	9028 (6)	2155 (22)	15.8 (12)
C(25) <i>A</i>	1137 (39)	9445 (12)	1496 (41)	23.7 (23)	C(25) <i>B</i>	5940 (40)	9417 (19)	1776 (63)	25.2 (29)
C(26) <i>A</i>	1218 (66)	9706 (15)	2149 (60)	41.7 (51)	C(26) <i>B</i>	6056 (65)	9406 (12)	717 (43)	37.9 (47)
C(27) <i>A</i>	-47 (36)	9362 (8)	652 (33)	29.4 (24)	C(27) <i>B</i>	4940 (56)	9487 (23)	1684 (77)	37.0 (48)
O(3) <i>C</i>	1448 (8)	4704 (3)	2746 (10)	10.4 (4)	O(3) <i>D</i>	1662 (8)	4779 (2)	7768 (9)	9.6 (4)
C(1) <i>C</i>	1153 (11)	3627 (4)	2766 (10)	7.6 (5)	C(1) <i>D</i>	1102 (9)	3690 (3)	7845 (8)	5.2 (4)
C(2) <i>C</i>	817 (10)	4038 (4)	2892 (10)	6.8 (5)	C(2) <i>D</i>	854 (10)	4113 (4)	7881 (11)	6.9 (5)
C(3) <i>C</i>	1767 (11)	4331 (4)	2675 (12)	8.0 (5)	C(3) <i>D</i>	1835 (10)	4380 (3)	7657 (11)	7.2 (5)
C(4) <i>C</i>	1956 (11)	4203 (4)	1475 (11)	8.2 (5)	C(4) <i>D</i>	2009 (9)	4255 (4)	6488 (10)	6.4 (5)
C(5) <i>C</i>	2174 (8)	3871 (3)	1366 (9)	5.5 (4)	C(5) <i>D</i>	2226 (10)	3833 (4)	6425 (10)	6.7 (5)
C(6) <i>C</i>	3047 (9)	3715 (3)	984 (10)	6.2 (4)	C(6) <i>D</i>	3080 (10)	3746 (4)	6010 (12)	8.2 (5)
C(7) <i>C</i>	3316 (11)	3318 (4)	756 (13)	8.8 (6)	C(7) <i>D</i>	3350 (10)	3339 (4)	5800 (10)	7.0 (5)
C(8) <i>C</i>	2380 (9)	2983 (3)	824 (10)	5.8 (4)	C(8) <i>D</i>	2383 (8)	3030 (3)	5844 (8)	5.0 (4)
C(9) <i>C</i>	1841 (8)	3105 (3)	1780 (9)	4.8 (4)	C(9) <i>D</i>	1868 (9)	3162 (3)	6817 (8)	5.1 (4)
C(10) <i>C</i>	1363 (8)	3475 (3)	1648 (8)	5.1 (4)	C(10) <i>D</i>	1381 (8)	3529 (3)	6676 (9)	4.7 (3)
C(11) <i>C</i>	1006 (11)	2755 (4)	1933 (11)	7.5 (5)	C(11) <i>D</i>	955 (10)	2808 (3)	6956 (9)	5.9 (4)
C(12) <i>C</i>	1497 (10)	2389 (4)	2052 (11)	7.2 (5)	C(12) <i>D</i>	1421 (10)	2437 (3)	7093 (9)	6.2 (4)
C(13) <i>C</i>	2026 (9)	2263 (3)	1113 (9)	5.3 (4)	C(13) <i>D</i>	1949 (10)	2308 (3)	6131 (9)	5.8 (4)
C(14) <i>C</i>	2846 (9)	2608 (3)	1011 (10)	6.1 (4)	C(14) <i>D</i>	2824 (9)	2669 (3)	6090 (10)	6.1 (4)
C(15) <i>C</i>	3510 (10)	2458 (4)	209 (10)	6.7 (5)	C(15) <i>D</i>	3512 (10)	2500 (4)	5329 (11)	7.5 (5)
C(16) <i>C</i>	3589 (13)	2054 (4)	507 (13)	9.6 (6)	C(16) <i>D</i>	3469 (10)	2075 (4)	5559 (12)	8.7 (6)
C(17) <i>C</i>	2773 (11)	1979 (3)	1321 (11)	7.4 (5)	C(17) <i>D</i>	2693 (10)	2007 (3)	6357 (11)	6.7 (5)
C(18) <i>C</i>	1187 (10)	2144 (4)	37 (10)	6.8 (5)	C(18) <i>D</i>	1131 (11)	2174 (4)	5016 (11)	7.6 (5)
C(19) <i>C</i>	321 (11)	3381 (4)	736 (11)	7.3 (5)	C(19) <i>D</i>	380 (10)	3463 (4)	5721 (10)	6.5 (4)
C(20) <i>C</i>	2266 (12)	1533 (4)	1189 (13)	9.6 (6)	C(20) <i>D</i>	2190 (12)	1589 (4)	6164 (12)	9.4 (6)
C(21) <i>C</i>	1480 (18)	1454 (5)	2013 (16)	13.7 (10)	C(21) <i>D</i>	1398 (15)	1480 (4)	6884 (15)	11.2 (8)
C(22) <i>C</i>	3258 (17)	1262 (7)	1307 (20)	16.1 (12)	C(22) <i>D</i>	3065 (15)	1310 (5)	6337 (19)	14.4 (10)
C(23) <i>C</i>	2681 (34)	849 (10)	781 (52)	37.4 (31)	C(23) <i>D</i>	2743 (24)	868 (6)	5757 (31)	23.9 (17)
C(24) <i>C</i>	3754 (49)	657 (10)	550 (48)	29.8 (30)	C(24) <i>D</i>	3834 (35)	744 (15)	5511 (53)	32.6 (32)
C(25) <i>C</i>	4187 (46)	707 (17)	-602 (67)	33.4 (39)	C(25) <i>D</i>	3952 (98)	620 (39)	4245 (94)	61.3 (99)
C(26) <i>C</i>	3427 (94)	521 (40)	-1529 (143)	128.5 (162)	C(26) <i>D</i>	3401 (89)	575 (41)	3630 (89)	60.5 (77)
C(27) <i>C</i>	4966 (48)	512 (15)	-463 (62)	39.3 (42)	C(27) <i>D</i>	4816 (57)	535 (20)	4566 (75)	58.5 (56)
O(3) <i>E</i>	3286 (8)	5288 (2)	7375 (9)	9.6 (4)	O(3) <i>F</i>	8324 (8)	5239 (3)	7598 (10)	10.9 (5)
C(1) <i>E</i>	2439 (10)	6254 (4)	8157 (11)	7.1 (5)	C(1) <i>F</i>	7391 (10)	6180 (4)	8138 (10)	7.3 (5)
C(2) <i>E</i>	2596 (10)	5837 (3)	8247 (11)	6.8 (5)	C(2) <i>F</i>	7569 (12)	5771 (4)	8308 (12)	8.9 (6)
C(3) <i>E</i>	3068 (10)	5676 (4)	7305 (10)	6.5 (5)	C(3) <i>F</i>	8121 (12)	5631 (4)	7371 (14)	10.0 (7)
C(4) <i>E</i>	4124 (10)	5920 (3)	7278 (11)	6.3 (4)	C(4) <i>F</i>	9238 (10)	5878 (4)	7500 (13)	8.6 (6)

Table 1 (cont.)

Triclinic form

	<i>x</i>	<i>y</i>	<i>z</i>	<i>B</i> _{eq} (Å ²)		<i>x</i>	<i>y</i>	<i>z</i>	<i>B</i> _{eq} (Å ²)
C(5)E	4055 (8)	6355 (3)	7258 (8)	4.4 (3)	C(5)F	9015 (9)	6283 (3)	7329 (10)	5.8 (4)
C(6)E	4395 (9)	6539 (3)	6483 (10)	6.1 (4)	C(6)F	9436 (10)	6475 (3)	6580 (9)	5.8 (4)
C(7)E	4393 (10)	6952 (4)	6414 (11)	6.8 (5)	C(7)F	0373 (10)	6886 (4)	6419 (9)	6.0 (4)
C(8)E	4071 (8)	7173 (3)	7447 (8)	4.3 (3)	C(8)F	9040 (9)	7105 (3)	7422 (10)	5.5 (4)
C(9)E	3147 (8)	6916 (3)	7773 (8)	4.7 (4)	C(9)F	8136 (9)	6860 (3)	7840 (9)	5.4 (4)
C(10)E	3498 (9)	6537 (3)	8131 (8)	5.1 (4)	C(10)F	8417 (9)	6485 (3)	8181 (8)	5.2 (4)
C(11)E	2693 (10)	7143 (3)	8701 (10)	5.8 (4)	C(11)F	7654 (10)	7103 (4)	8740 (10)	6.6 (5)
C(12)E	2425 (10)	7532 (4)	8434 (10)	6.8 (5)	C(12)F	7403 (9)	7481 (3)	8416 (10)	5.9 (4)
C(13)E	3382 (8)	7781 (3)	8120 (8)	4.5 (3)	C(13)F	8343 (9)	7737 (3)	8091 (9)	5.9 (4)
C(14)E	3667 (9)	7537 (3)	7164 (9)	5.4 (4)	C(14)F	8681 (9)	7469 (3)	7168 (9)	5.7 (4)
C(15)E	4439 (10)	7832 (4)	6695 (10)	6.7 (5)	C(15)F	9445 (10)	7770 (3)	6686 (10)	6.1 (4)
C(16)E	3958 (11)	8208 (4)	6882 (12)	7.7 (5)	C(16)F	8990 (11)	8154 (4)	6761 (11)	7.7 (5)
C(17)E	3085 (10)	8131 (3)	7541 (10)	6.2 (4)	C(17)F	8074 (9)	8073 (3)	7488 (11)	6.8 (5)
C(18)E	4302 (11)	7920 (4)	9164 (11)	8.4 (6)	C(18)F	9286 (10)	7887 (4)	9155 (10)	7.4 (5)
C(19)E	4277 (11)	6612 (4)	9283 (10)	6.9 (5)	C(19)F	9182 (12)	6559 (4)	9350 (10)	8.0 (5)
C(20)E	2981 (10)	8512 (4)	8292 (12)	8.0 (5)	C(20)F	8023 (14)	8468 (4)	8160 (14)	10.2 (7)
C(21)E	2208 (11)	8449 (4)	9064 (13)	8.7 (6)	C(21)F	7253 (13)	8428 (4)	8960 (13)	10.1 (7)
C(22)E	2529 (19)	8792 (5)	7379 (17)	14.2 (10)	C(22)F	7524 (20)	8736 (5)	7287 (17)	14.8 (10)
C(23)E	2437 (25)	9178 (7)	7813 (25)	18.8 (15)	C(23)F	7571 (26)	9132 (7)	7733 (25)	19.2 (15)
C(24)E	2137 (36)	9426 (12)	6911 (38)	22.1 (23)	C(24)F	7095 (29)	9350 (8)	6795 (28)	17.7 (16)
C(25)E	1016 (43)	9366 (13)	6368 (44)	24.1 (27)	C(25)F	5767 (38)	9274 (10)	6479 (43)	22.6 (21)
C(26)E	457 (47)	9478 (18)	7238 (51)	36.5 (41)	C(26)F	5752 (52)	9615 (15)	7483 (50)	37.1 (43)
C(27)E	929 (39)	9731 (13)	5761 (38)	35.3 (33)	C(27)F	5706 (44)	9482 (18)	5488 (40)	35.8 (36)
O(3)G	6244 (8)	4681 (3)	2048 (9)	10.4 (4)	O(3)H	6486 (7)	4714 (2)	7236 (8)	9.0 (4)
C(1)G	7315 (12)	3737 (4)	1684 (10)	7.7 (5)	C(1)H	7337 (11)	3736 (4)	6704 (11)	7.5 (5)
C(2)G	7263 (12)	4175 (4)	1741 (11)	8.0 (5)	C(2)H	7404 (10)	4194 (4)	6806 (10)	7.0 (5)
C(3)G	6187 (11)	4274 (4)	2067 (13)	8.6 (6)	C(3)H	6388 (10)	4308 (4)	7114 (11)	6.8 (5)
C(4)G	6090 (11)	4162 (4)	3125 (12)	8.4 (6)	C(4)H	6206 (10)	4172 (4)	8188 (11)	7.2 (5)
C(5)G	6161 (8)	3726 (3)	3166 (9)	4.8 (4)	C(5)H	6252 (9)	3749 (4)	8213 (10)	6.6 (4)
C(6)G	5421 (10)	3511 (4)	3543 (11)	7.3 (5)	C(6)H	5453 (9)	3503 (4)	8529 (10)	6.9 (5)
C(7)G	5403 (10)	3094 (4)	3627 (11)	7.1 (5)	C(7)H	5412 (9)	3084 (4)	8611 (11)	6.8 (5)
C(8)G	6468 (8)	2960 (3)	3494 (8)	4.6 (4)	C(8)H	6498 (8)	2961 (3)	8455 (9)	5.0 (4)
C(9)G	6912 (9)	3140 (3)	2570 (9)	5.6 (4)	C(9)H	6934 (8)	3140 (3)	7552 (8)	4.5 (3)
C(10)G	7123 (9)	3594 (3)	2801 (9)	5.6 (4)	C(10)H	7190 (9)	3585 (3)	7814 (8)	5.3 (4)
C(11)G	7845 (11)	2969 (4)	2268 (10)	7.7 (5)	C(11)H	7967 (10)	2975 (4)	7335 (10)	6.8 (5)
C(12)G	7667 (11)	2526 (4)	2068 (10)	7.0 (5)	C(12)H	7729 (10)	2525 (4)	7082 (9)	6.7 (5)
C(13)G	7331 (10)	2361 (3)	3049 (9)	6.0 (4)	C(13)H	7348 (9)	2356 (3)	8063 (8)	4.9 (4)
C(14)G	6277 (9)	2521 (4)	3226 (9)	6.4 (4)	C(14)H	6309 (8)	2522 (3)	8159 (9)	5.3 (4)
C(15)G	5791 (10)	2276 (4)	3973 (11)	7.6 (5)	C(15)H	5745 (10)	2263 (4)	8890 (11)	6.9 (5)
C(16)G	6068 (11)	1869 (4)	3705 (13)	8.7 (6)	C(16)H	6136 (10)	1869 (4)	8666 (13)	8.6 (6)
C(17)G	6886 (11)	1918 (4)	2833 (10)	7.3 (5)	C(17)H	6871 (10)	1916 (4)	7833 (10)	7.0 (5)
C(18)G	8257 (9)	2461 (4)	4095 (10)	6.3 (4)	C(18)H	8227 (10)	2468 (4)	9126 (10)	6.4 (4)
C(19)G	8139 (9)	3771 (3)	3746 (9)	5.4 (4)	C(19)H	8191 (9)	3747 (3)	8746 (10)	6.2 (4)
C(20)G	7666 (13)	1640 (4)	2886 (13)	9.4 (6)	C(20)H	7648 (11)	1628 (4)	7849 (12)	8.3 (5)
C(21)G	8419 (18)	1677 (5)	2064 (18)	14.7 (10)	C(21)H	8448 (17)	1665 (5)	7041 (16)	12.9 (9)
C(22)G	7016 (19)	1217 (5)	2708 (23)	17.3 (12)	C(22)H	7010 (19)	1199 (5)	7666 (21)	16.0 (11)
C(23)G	7794 (23)	895 (7)	2775 (28)	17.1 (14)	C(23)H	7629 (25)	874 (7)	7685 (26)	18.0 (14)
C(24)G	8184 (32)	872 (11)	3925 (25)	22.6 (20)	C(24)H	8305 (23)	915 (9)	8881 (25)	18.3 (15)
C(25)G	8795 (33)	527 (13)	4326 (55)	24.7 (27)	C(25)H	8617 (52)	472 (19)	8991 (58)	28.6 (39)
C(26)G	8018 (51)	199 (18)	4564 (56)	37.4 (43)	C(26)H	8701 (70)	415 (21)	10000 (46)	45.8 (55)
C(27)G	9618 (43)	556 (14)	3826 (56)	35.6 (40)	C(27)H	9704 (56)	583 (18)	8667 (64)	34.3 (45)
C(1)E1	4243 (13)	4924 (5)	137 (14)	11.3 (7)	C(1)E2	10336 (17)	5077 (7)	4941 (18)	17.2 (12)
C(2)E1	5047 (15)	5126 (5)	-252 (14)	12.2 (8)	C(2)E2	9618 (25)	4907 (10)	5292 (25)	24.8 (19)
OE1	4480 (7)	4981 (3)	1361 (7)	8.8 (4)	OE2	9866 (10)	4950 (3)	3651 (9)	11.9 (5)
C(1)E3	4344 (16)	4970 (7)	5243 (14)	14.9 (10)	C(1)E4	10244 (17)	5087 (6)	9832 (18)	15.2 (10)
C(2)E3	5119 (18)	5038 (10)	4751 (23)	22.8 (17)	C(2)E4	9331 (19)	4980 (7)	10315 (16)	16.6 (11)
OE3	4637 (8)	4928 (3)	6423 (8)	9.5 (4)	OE4	10045 (10)	5003 (3)	8698 (9)	11.4 (5)

Table 1 (cont.)

Monoclinic form

	<i>x</i>	<i>y</i>	<i>z</i>	<i>B</i> _{eq} (Å ²)		<i>x</i>	<i>y</i>	<i>z</i>	<i>B</i> _{eq} (Å ²)
O(3)A	1742 (11)	2620 (2)	3133 (13)	11.3 (6)	O(3)B	6725 (10)	2588 (2)	3643 (12)	10.7 (6)
C(1)A	1593 (11)	3141 (2)	2195 (13)	5.7 (6)	C(1)B	6684 (12)	3115 (3)	2700 (15)	8.1 (7)
C(2)A	1782 (11)	2913 (2)	2193 (14)	5.8 (6)	C(2)B	6944 (16)	2883 (3)	2678 (18)	9.6 (9)
C(3)A	1693 (12)	2828 (2)	3255 (13)	5.6 (6)	C(3)B	6548 (14)	2801 (3)	3716 (15)	7.8 (7)
C(4)A	544 (13)	2858 (3)	3509 (15)	7.0 (7)	C(4)B	5319 (12)	2847 (3)	3645 (18)	8.7 (8)
C(5)A	215 (10)	3075 (2)	3395 (10)	3.8 (4)	C(5)B	5135 (11)	3064 (3)	3586 (14)	6.5 (6)
C(6)A	-289 (12)	3158 (2)	4191 (12)	5.6 (6)	C(6)B	4610 (12)	3142 (3)	4289 (13)	6.2 (6)
C(7)A	-566 (10)	3353 (2)	4260 (12)	4.5 (5)	C(7)B	4222 (13)	3353 (3)	4246 (14)	6.9 (6)
C(8)A	-619 (13)	3468 (3)	3097 (15)	7.7 (7)	C(8)B	4413 (10)	3453 (2)	3166 (10)	3.7 (5)
C(9)A	423 (12)	3417 (2)	2695 (14)	6.0 (6)	C(9)B	5439 (11)	3393 (2)	2809 (12)	4.7 (5)
C(10)A	467 (12)	3188 (3)	2411 (12)	6.0 (6)	C(10)B	5488 (10)	3169 (2)	2674 (12)	4.9 (5)
C(11)A	569 (12)	3537 (2)	1660 (13)	5.3 (5)	C(11)B	5678 (13)	3514 (3)	1777 (13)	7.1 (7)
C(12)A	479 (11)	3765 (2)	1911 (11)	5.1 (5)	C(12)B	5562 (11)	3715 (2)	1926 (13)	5.2 (5)
C(13)A	-589 (11)	3817 (2)	2244 (11)	4.1 (5)	C(13)B	4525 (11)	3784 (2)	2255 (12)	5.2 (5)
C(14)A	-595 (11)	3697 (2)	3281 (12)	5.1 (5)	C(14)B	4368 (11)	3663 (2)	3219 (13)	5.7 (6)
C(15)A	-1499 (13)	3767 (3)	3767 (14)	6.9 (7)	C(15)B	3411 (14)	3770 (2)	3633 (18)	8.3 (8)
C(16)A	-1524 (14)	3994 (3)	3457 (16)	8.4 (8)	C(16)B	3481 (13)	3978 (2)	3323 (14)	6.5 (6)
C(17)A	-600 (13)	4010 (3)	2773 (13)	6.6 (6)	C(17)B	4413 (12)	3996 (2)	2659 (12)	5.9 (6)
C(18)A	-1518 (13)	3766 (3)	1348 (13)	6.6 (6)	C(18)B	3613 (11)	3759 (3)	1210 (13)	6.0 (6)
C(19)A	-387 (15)	3135 (3)	1387 (15)	9.3 (8)	C(19)B	4789 (13)	3104 (3)	1510 (17)	9.0 (8)
C(20)A	-735 (13)	4184 (2)	1988 (14)	6.4 (6)	C(20)B	4284 (16)	4174 (3)	1845 (18)	9.3 (8)
C(21)A	194 (26)	4209 (4)	1384 (24)	16.8 (15)	C(21)B	5248 (23)	4177 (4)	1282 (22)	14.4 (12)
C(22)A	-1018 (21)	4372 (3)	2516 (22)	13.6 (12)	C(22)B	4018 (18)	4342 (3)	2422 (17)	10.0 (9)
C(23)A	-1243 (25)	4562 (4)	1798 (34)	17.3 (17)	C(23)B	3900 (20)	4544 (3)	1714 (23)	11.1 (10)
C(24)A	-2249 (27)	4539 (5)	930 (31)	15.4 (16)	C(24)B	2782 (30)	4499 (4)	843 (26)	15.1 (15)
C(25)A	-2732 (63)	4744 (8)	386 (53)	29.3 (35)	C(25)B	2294 (30)	4721 (7)	361 (31)	18.9 (19)
C(26)A	-2356 (71)	4891 (9)	380 (68)	41.9 (48)	C(26)B	2998 (38)	4758 (5)	-586 (50)	27.8 (32)
C(27)A	-3345 (47)	4679 (5)	-616 (32)	29.0 (29)	C(27)B	1312 (37)	4708 (7)	-289 (47)	28.3 (29)
O(3)C	383 (10)	2359 (2)	3574 (13)	10.6 (6)	O(3)D	539 (9)	2390 (2)	8550 (12)	10.2 (6)
C(1)C	647 (12)	1820 (2)	4181 (13)	5.9 (6)	C(1)D	587 (14)	1859 (4)	9125 (16)	10.2 (9)
C(2)C	136 (16)	2017 (3)	4007 (16)	9.3 (8)	C(2)D	112 (11)	2053 (2)	9047 (14)	5.8 (6)
C(3)C	949 (19)	2168 (3)	3740 (21)	12.7 (11)	C(3)D	941 (12)	2195 (3)	8624 (16)	7.6 (7)
C(4)C	1178 (11)	2106 (2)	2563 (12)	5.7 (6)	C(4)D	1271 (15)	2127 (3)	7627 (18)	9.8 (8)
C(5)C	1621 (12)	1890 (2)	2653 (13)	5.5 (5)	C(5)D	1598 (12)	1931 (3)	7615 (12)	6.6 (6)
C(6)C	2513 (12)	1855 (3)	2323 (16)	8.5 (8)	C(6)D	2557 (12)	1866 (3)	7320 (14)	6.7 (6)
C(7)C	2988 (12)	1663 (3)	2286 (14)	6.9 (7)	C(7)D	3054 (14)	1666 (3)	7369 (14)	8.5 (8)
C(8)C	2247 (11)	1497 (2)	2519 (12)	4.7 (5)	C(8)D	2236 (12)	1518 (2)	7527 (14)	6.5 (6)
C(9)C	1707 (12)	1547 (3)	3509 (13)	6.5 (6)	C(9)D	1544 (10)	1581 (2)	8377 (9)	3.3 (4)
C(10)C	978 (12)	1734 (2)	3090 (11)	4.9 (5)	C(10)D	942 (11)	1772 (2)	8055 (13)	5.4 (6)
C(11)C	970 (14)	1389 (3)	3747 (14)	7.8 (7)	C(11)D	876 (13)	1404 (3)	8688 (15)	7.6 (7)
C(12)C	1693 (15)	1197 (3)	4078 (14)	7.6 (7)	C(12)D	1510 (13)	1229 (3)	9054 (13)	6.6 (6)
C(13)C	2228 (13)	1136 (3)	3130 (14)	7.0 (7)	C(13)D	2175 (12)	1159 (2)	8169 (13)	5.7 (6)
C(14)C	2897 (11)	1309 (2)	2906 (13)	4.9 (5)	C(14)D	2807 (11)	1336 (2)	7919 (11)	5.1 (5)
C(15)C	3664 (14)	1235 (3)	2207 (14)	7.9 (7)	C(15)D	3642 (12)	1254 (3)	7226 (14)	7.9 (7)
C(16)C	3900 (14)	1027 (3)	2635 (16)	8.5 (8)	C(16)D	3784 (14)	1033 (3)	7696 (17)	9.3 (8)
C(17)C	3106 (13)	994 (2)	3506 (14)	6.5 (6)	C(17)D	3073 (15)	1011 (3)	8540 (15)	8.0 (7)
C(18)C	1493 (13)	1055 (3)	2130 (14)	6.6 (6)	C(18)D	1384 (14)	1090 (3)	7097 (14)	7.3 (7)
C(19)C	-16 (12)	1697 (3)	2226 (13)	7.0 (6)	C(19)D	-40 (11)	1733 (3)	7196 (12)	6.1 (6)
C(20)C	2876 (16)	770 (3)	3625 (16)	9.3 (8)	C(20)D	2772 (14)	790 (3)	8475 (17)	9.0 (8)
C(21)C	2150 (20)	736 (3)	4380 (21)	12.4 (11)	C(21)D	2010 (21)	743 (4)	9374 (21)	13.2 (11)
C(22)C	3950 (21)	630 (4)	3659 (36)	20.8 (20)	C(22)D	3795 (18)	654 (3)	8919 (20)	11.9 (10)
C(23)C	3719 (33)	419 (5)	3514 (46)	29.9 (28)	C(23)D	3562 (25)	447 (4)	8358 (32)	23.6 (19)
C(24)C	4940 (56)	347 (8)	3198 (93)	33.2 (50)	C(24)D	4892 (57)	331 (7)	8545 (54)	30.6 (35)
C(25)C	5201 (80)	279 (16)	2195 (118)	36.6 (62)	C(25)D	4838 (61)	302 (12)	7186 (96)	33.6 (44)
C(26)C	5476 (196)	434 (26)	1663 (235)	123.0 (261)	C(26)D	5719 (102)	446 (16)	7223 (124)	56.7 (87)
C(27)C	6329 (73)	229 (10)	2691 (71)	36.7 (43)	C(27)D	6220 (60)	202 (7)	8055 (59)	38.5 (40)
O(3)E	1903 (9)	2639 (2)	7892 (11)	9.3 (5)	O(3)F	7026 (10)	2626 (2)	8159 (13)	11.4 (6)
C(1)E	576 (12)	3135 (2)	8239 (16)	7.2 (7)	C(1)F	5530 (13)	3093 (3)	8230 (16)	8.5 (8)
C(2)E	981 (14)	2911 (3)	8517 (15)	8.5 (8)	C(2)F	5924 (13)	2886 (3)	8707 (16)	7.7 (7)
C(3)E	1463 (14)	2829 (3)	7568 (14)	6.9 (6)	C(3)F	6609 (15)	2813 (3)	7847 (17)	9.2 (8)
C(4)E	2469 (11)	2962 (2)	7528 (14)	5.4 (6)	C(4)F	7578 (17)	2939 (3)	7717 (17)	9.8 (9)
C(5)E	2141 (11)	3179 (3)	7315 (14)	6.6 (6)	C(5)F	7149 (12)	3145 (2)	7410 (13)	6.2 (6)

Table 1 (cont.)

Monoclinic form

	<i>x</i>	<i>y</i>	<i>z</i>	B_{eq} (\AA^2)		<i>x</i>	<i>y</i>	<i>z</i>	B_{eq} (\AA^2)
C(6)E	2376 (12)	3280 (3)	6449 (13)	6.6 (6)	C(6)F	7430 (12)	3241 (2)	6522 (14)	6.3 (6)
C(7)E	2159 (13)	3486 (3)	6188 (13)	6.7 (6)	C(7)F	7186 (13)	3457 (3)	6190 (14)	7.4 (7)
C(8)E	1756 (11)	3591 (2)	7091 (13)	5.7 (6)	C(8)F	6758 (9)	3565 (2)	7155 (12)	4.4 (5)
C(9)E	959 (11)	3459 (2)	7609 (12)	4.9 (5)	C(9)F	5928 (11)	3441 (3)	7583 (12)	5.6 (6)
C(10)E	1460 (11)	3274 (2)	8106 (13)	5.7 (6)	C(10)F	6422 (11)	3245 (2)	8106 (11)	5.1 (5)
C(11)E	353 (14)	3570 (3)	8379 (14)	6.7 (6)	C(11)F	5424 (12)	3554 (3)	8429 (14)	6.5 (6)
C(12)E	-134 (12)	3768 (3)	7926 (15)	7.2 (7)	C(12)F	4949 (11)	3742 (2)	7916 (12)	5.2 (5)
C(13)E	723 (12)	3897 (2)	7523 (13)	5.7 (6)	C(13)F	5720 (10)	3866 (2)	7427 (11)	4.5 (5)
C(14)E	1170 (12)	3770 (2)	6679 (12)	5.5 (6)	C(14)F	6185 (11)	3739 (2)	6675 (11)	4.6 (5)
C(15)E	1759 (13)	3924 (2)	6049 (13)	6.3 (6)	C(15)F	6810 (13)	3880 (3)	6054 (14)	6.9 (7)
C(16)E	1111 (14)	4107 (3)	6072 (16)	8.0 (7)	C(16)F	6162 (13)	4072 (3)	5984 (18)	8.5 (8)
C(17)E	233 (12)	4065 (2)	6782 (14)	6.3 (6)	C(17)F	5314 (13)	4039 (3)	6757 (15)	7.1 (7)
C(18)E	1558 (12)	3959 (3)	8432 (14)	7.0 (6)	C(18)F	6562 (15)	3944 (3)	8468 (16)	8.5 (8)
C(19)E	2279 (14)	3303 (3)	9272 (15)	8.3 (7)	C(19)F	7153 (14)	3292 (3)	9288 (15)	8.7 (8)
C(20)E	-30 (13)	4258 (3)	7269 (16)	7.7 (7)	C(20)F	5057 (20)	4237 (3)	7311 (22)	13.3 (12)
C(21)E	-843 (15)	4236 (3)	8066 (16)	9.2 (9)	C(21)F	4257 (15)	4222 (2)	8128 (17)	8.7 (8)
C(22)E	-754 (21)	4396 (3)	6209 (21)	13.2 (12)	C(22)F	4564 (30)	4407 (5)	6497 (35)	24.4 (23)
C(23)E	-864 (30)	4599 (4)	6508 (29)	21.5 (18)	C(23)F	3954 (34)	4548 (7)	6378 (45)	30.5 (29)
C(24)E	-1457 (23)	4692 (4)	5325 (26)	13.3 (12)	C(24)F	3493 (45)	4639 (7)	5152 (50)	23.6 (27)
C(25)E	-2593 (41)	4680 (7)	5188 (41)	24.9 (25)	C(25)F	2357 (72)	4643 (11)	4953 (61)	29.1 (38)
C(26)E	-3058 (43)	4833 (12)	5655 (58)	36.6 (43)	C(26)F	1995 (40)	4768 (9)	5763 (41)	31.8 (32)
C(27)E	-2865 (45)	4829 (9)	4064 (46)	40.3 (38)	C(27)F	2469 (64)	4817 (13)	4241 (54)	42.8 (55)
O(3)G	5186 (10)	2344 (2)	2911 (12)	10.3 (6)	O(3)H	5420 (10)	2364 (2)	8078 (11)	9.2 (5)
C(1)G	6720 (15)	1879 (3)	3000 (14)	8.1 (7)	C(1)H	6794 (13)	1882 (3)	8060 (13)	7.0 (7)
C(2)G	6530 (14)	2102 (3)	2873 (14)	7.9 (7)	C(2)H	6636 (13)	2098 (2)	7906 (14)	6.4 (6)
C(3)G	5472 (14)	2140 (3)	3051 (15)	7.7 (7)	C(3)H	5462 (16)	2151 (3)	8124 (19)	11.0 (9)
C(4)G	5306 (13)	2083 (2)	4229 (16)	7.5 (7)	C(4)H	5477 (12)	2098 (3)	9356 (15)	7.8 (7)
C(5)G	5569 (12)	1878 (3)	4529 (13)	7.3 (7)	C(5)H	5696 (11)	1871 (2)	9492 (12)	5.8 (6)
C(6)G	4991 (13)	1757 (3)	4937 (15)	7.8 (7)	C(6)H	5011 (12)	1758 (3)	9987 (14)	6.4 (6)
C(7)G	5160 (12)	1548 (3)	5246 (15)	7.5 (7)	C(7)H	5242 (12)	1547 (2)	10233 (14)	6.5 (6)
C(8)G	6317 (12)	1488 (2)	5211 (12)	5.7 (6)	C(8)H	6357 (10)	1482 (2)	10188 (11)	4.6 (5)
C(9)G	6644 (12)	1580 (2)	4181 (14)	6.4 (6)	C(9)H	6696 (12)	1573 (2)	9175 (12)	5.6 (5)
C(10)G	6657 (11)	1804 (2)	4190 (12)	5.3 (5)	C(10)H	6742 (11)	1796 (3)	9272 (12)	5.7 (6)
C(11)G	7751 (13)	1485 (3)	4004 (12)	6.7 (6)	C(11)H	7816 (12)	1489 (2)	9053 (14)	6.2 (6)
C(12)G	7798 (12)	1266 (2)	3997 (13)	6.1 (6)	C(12)H	7867 (15)	1267 (3)	9035 (16)	8.8 (8)
C(13)G	7500 (11)	1180 (2)	5088 (11)	4.0 (5)	C(13)H	7503 (13)	1183 (2)	9993 (14)	5.8 (6)
C(14)G	6399 (12)	1262 (3)	5160 (14)	6.7 (6)	C(14)H	6396 (10)	1263 (2)	10063 (11)	4.4 (5)
C(15)G	6076 (12)	1142 (3)	6029 (14)	7.3 (7)	C(15)H	6007 (13)	1137 (3)	11021 (16)	8.4 (8)
C(16)G	6570 (13)	935 (3)	5950 (15)	7.2 (7)	C(16)H	6495 (13)	936 (3)	10821 (17)	8.8 (8)
C(17)G	7262 (13)	960 (2)	5073 (15)	7.2 (7)	C(17)H	7285 (13)	965 (3)	10019 (14)	7.3 (7)
C(18)G	8339 (12)	1243 (3)	6073 (13)	6.8 (6)	C(18)H	8343 (12)	1239 (3)	11105 (14)	6.8 (6)
C(19)G	7566 (13)	1874 (3)	5027 (16)	7.4 (7)	C(19)H	7623 (12)	1884 (2)	10095 (12)	5.2 (5)
C(20)G	8172 (15)	824 (3)	5232 (15)	9.4 (8)	C(20)H	8180 (15)	815 (3)	10209 (17)	8.9 (8)
C(21)G	8923 (18)	846 (4)	4393 (18)	12.3 (10)	C(21)H	8949 (21)	843 (3)	9387 (19)	12.8 (11)
C(22)G	7774 (20)	610 (4)	5272 (29)	16.2 (15)	C(22)H	7835 (20)	603 (4)	10169 (21)	14.1 (12)
C(23)G	8578 (23)	436 (4)	5400 (30)	17.2 (15)	C(23)H	8580 (37)	435 (7)	10495 (40)	28.6 (29)
C(24)G	9078 (26)	445 (5)	6544 (25)	18.1 (15)	C(24)H	9185 (30)	455 (6)	11599 (32)	19.4 (18)
C(25)G	9989 (39)	223 (8)	7517 (83)	30.0 (37)	C(25)H	9708 (38)	229 (7)	12207 (65)	24.4 (25)
C(26)G	10835 (128)	357 (17)	7610 (128)	59.8 (112)	C(26)H	10612 (100)	321 (15)	13027 (91)	54.4 (81)
C(27)G	10840 (75)	270 (11)	6343 (53)	33.8 (39)	C(27)H	10950 (53)	303 (6)	11603 (44)	26.3 (29)
C(1)E1	3140 (17)	2456 (4)	854 (23)	13.6 (12)	C(1)E2	9067 (17)	2534 (4)	5497 (25)	15.8 (13)
C(2)E1	3854 (18)	2554 (3)	390 (16)	11.8 (10)	C(2)E2	8408 (21)	2449 (5)	6038 (23)	18.2 (16)
OE1	3273 (9)	2493 (2)	2059 (10)	10.5 (6)	OE2	8704 (11)	2477 (3)	4387 (10)	12.3 (6)
C(1)E3	3089 (26)	2472 (6)	6050 (26)	20.8 (19)	C(1)E4	8978 (21)	2548 (5)	10506 (26)	19.7 (17)
C(2)E3	3665 (26)	2494 (6)	5473 (28)	24.8 (22)	C(2)E4	8160 (23)	2482 (5)	11112 (22)	17.6 (15)
OE3	3441 (10)	2471 (2)	7181 (11)	10.4 (6)	OE4	8783 (11)	2949 (2)	9406 (12)	12.0 (6)

dent cholesterol molecules are labelled *A*, *B*, ..., *H*. This labelling is the same as that used for cholesterol monohydrate (Craven, 1979) to whose structure the hemiethanolate structures bear a remarkable resemblance.

The overall structures of the hemiethanolates are shown in Fig. 1. Both are characteristic bilayer structures with alternating hydrophilic and hydrophobic layers. The only significant difference in molecular packing in the two structures is in the

hydrophobic region, where the end-for-end interaction of neighboring molecules is different. While the long directions of the molecules are roughly parallel in the triclinic form, there is a distinct kink, at the hydrophobic contact, in the monoclinic form. Unlike the situation in anhydrous cholesterol (Shieh, Hoard & Nordman, 1977a, 1981) there is no interdigititation of side chains in the hemiethanolates.

Two chains of hydrogen bonds, running in the α direction, link the cholesterol and ethanol molecules in the hydrophilic region, as shown in Fig. 2. Hydrogen-

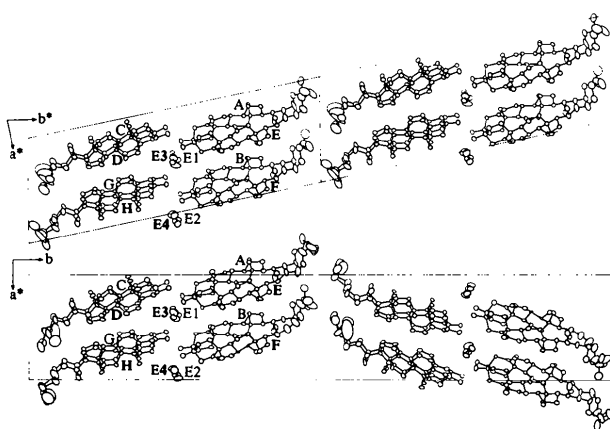


Fig. 1. Two cells of the triclinic form of cholesterol hemiethanolate (top), compared to one cell of the monoclinic form (bottom). Each structure is viewed in a direction 5° from the c axis, showing the pseudosymmetry which relates molecules C and G to D and H by a $c/2$ translation. The relationship of A and E to B and F by an $a/2$ translation can also be seen. $E1, \dots, E4$ are the four ethanol molecules. The C and O atoms are shown as 10% probability thermal ellipsoids.

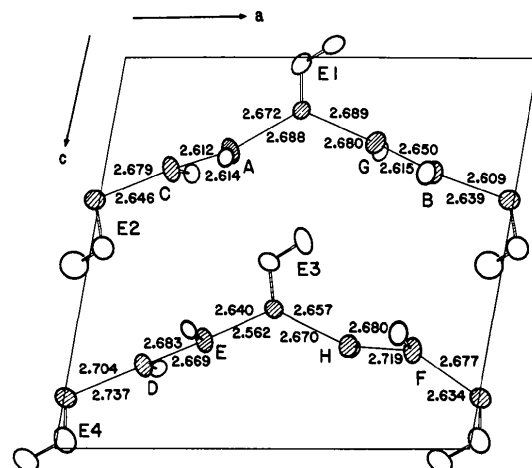


Fig. 2. Hydrogen bonding in the cholesterol hemiethanolate structures. The O atoms (shaded) of the cholesterol molecules A, \dots, H are shown with their adjacent $C(3)$ atoms. $E1, \dots, E4$ are ethanol molecules. Hydrogen-bond lengths in Å (e.s.d. 0.020 Å) are given, for the triclinic form, above the bond and, for the monoclinic form, below.

bond distances in the two structures are shown separately; their differences are small and probably not significant.

The close similarity between the hemiethanolate and the monohydrate structures is remarkable, especially in view of their totally different hydrogen-bonding patterns. The hydrogen bonds in the monohydrate form a two-dimensional sheet involving the eight water molecules in the hydrophilic region of the cell (Craven, 1976, especially Fig. 2), while the four ethanol molecules in the hemiethanolates participate in one-dimensional hydrogen-bonded chains (Fig. 2). Despite this difference, the lateral packing of steroid skeletons is nearly identical in the two structures. This can be seen by comparing our Fig. 1 with Fig. 1 of Craven's (1976) paper.

Fig. 3 shows part of the triclinic hemiethanolate structure viewed along the pseudo-twofold axes, which are directed along [101]. This figure is to be compared with Fig. 3 of Craven's (1979) second paper, showing the corresponding view of the monohydrate structure. The comparison shows a sideways displacement of the molecules (G, D) on one side of the hydrophilic region relative to those (A, F) on the other side, but a very close similarity in the packing of molecules on each side. With the exception of molecule D , the side-chain conformations are also very similar.

The most striking demonstration of the similarity of the cholesterol packing in the hemiethanolate and the monohydrate structures is the least-squares superposition of the two. Superposing the 84-atom rigid unit consisting of atoms $O(3), C(1), \dots, C(20)$ of molecules A, B, E and F of the monohydrate onto the corresponding unit of the (triclinic) hemiethanolate gives an r.m.s. atom–atom misfit of only 0.324 \AA . Similarly, the corresponding 84-atom unit of $C, D, G,$

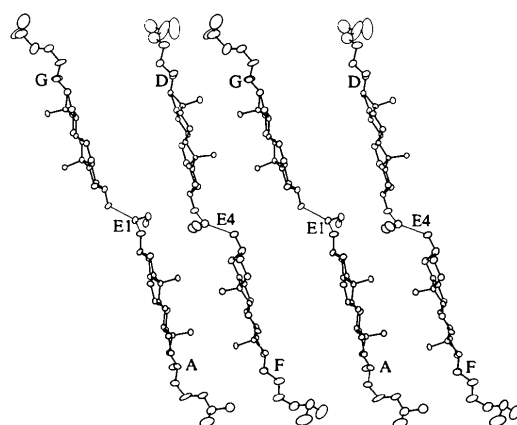


Fig. 3. View of one half of the triclinic cholesterol hemiethanolate structure along the [101] axis. Approximate twofold symmetry, relating molecules A to G and F to D , can be seen in the packing of the steroid skeletons. Molecules are labelled as in Figs. 1 and 2.

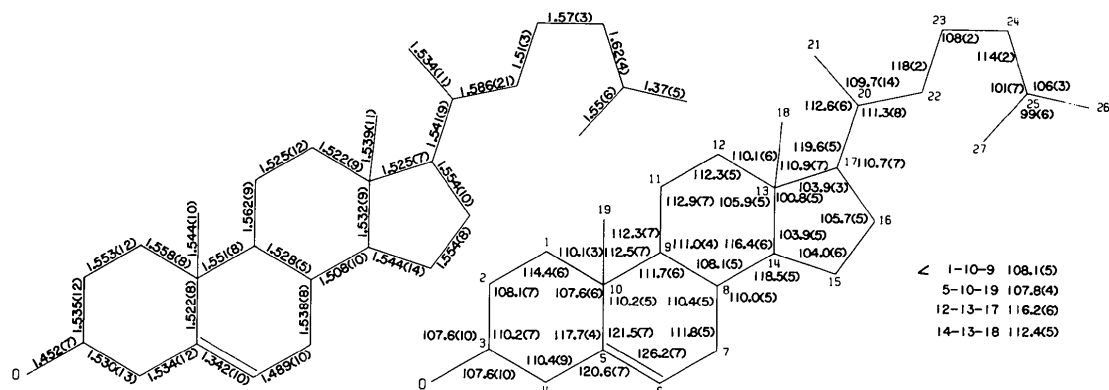


Fig. 4. Bond distances (\AA) (left) and angles ($^\circ$) (right) given as means, and standard deviations of the means of values from the 16 independent cholesterol molecules in the triclinic and monoclinic hemiethanolate structures.

H of the monohydrate superposes on the hemiethanolate with only 0.566 \AA r.m.s. misfit. Molecule D with a 0.796 \AA r.m.s. misfit is the worst-fitting part of this 84-atom unit. This is also reflected in Fig. 3, where a comparison with the corresponding figure for the monohydrate (Craven, 1979, Fig. 3) shows a slight tilt of the D molecules. Nonetheless, the closeness of fit of these large structural units is remarkable. Clearly, the lateral displacement, mentioned in the discussion of Fig. 3, precludes any equally close fitting of all eight cholesterol units in the cell.

Bond distances and angles, averaged over the 16 independent molecules, are shown in Fig. 4. The accuracy of these parameters in the side chains is low, especially at the ends of the chains, as the thermal motion (Table 1) is very strong. This tendency is even more marked in the hemiethanolate structures than in the monohydrate or the anhydrous forms of cholesterol. The terminal side-chain atoms C(26) of molecule C in both structures show exceptionally large positional standard deviations of up to 0.25 \AA , and unreasonably high values of B_{ij} . This behavior suggests a possible disorder involving a rotation about the C(24)–C(25) bond; such a disorder could leave the site of C(27) essentially fully occupied, while distributing

C(26) over two, perhaps unequally occupied sites. However, in view of the low accuracy of all side-chain parameters, and in the absence of clearly discernible alternative carbon site peaks in difference electron density maps, least-squares refinement of a partial-occupancy model was deemed unwarranted.

This work was supported by Grant GM 15259 from the National Institutes of Health.

References

- CRAVEN, B. M. (1976). *Nature (London)*, **260**, 727–729.
- CRAVEN, B. M. (1979). *Acta Cryst. B* **35**, 1123–1128.
- HOARD, L. G. & NORDMAN, C. E. (1979). *Acta Cryst. A* **35**, 1010–1015.
- SCHILLING, J. W. (1970). *Crystallographic Computing*, edited by F. R. AHMED, pp. 115–123. Copenhagen: Munksgaard.
- SHIEH, H.-S., HOARD, L. G. & NORDMAN, C. E. (1977a). *Nature (London)*, **267**, 287–289.
- SHIEH, H.-S., HOARD, L. G. & NORDMAN, C. E. (1977b). *Am. Crystallogr. Assoc. Abstr. Ser. 2*, **5**, 30.
- SHIEH, H.-S., HOARD, L. G. & NORDMAN, C. E. (1981). *Acta Cryst. B* **37**, 1538–1543.
- ZACHARIASEN, W. H. (1968). *Acta Cryst. A* **24**, 212–216.